

Published in final edited form as:

Pharm Res. 2008 September ; 25(9): 2074–2082. doi:10.1007/s11095-008-9603-6.

Doxorubicin Loaded pH-sensitive Micelle: Antitumoral Efficacy against Ovarian A2780/DOX^R Tumor

Dongin Kim¹, Eun Seong Lee¹, Kyeongsoon Park², Ick Chan Kwon², and You Han Bae^{1,3}

¹ Department of Pharmaceutics and Pharmaceutical Chemistry, University of Utah, 421 Wakara Way, Suite 318, Salt Lake City, Utah 84108, USA.

² Biomedical Research Center, Korea Institute of Science and Technology, 39–1 Hawolgok-dong, Seongbuk-gu, Seoul 136–791, South Korea.

Abstract

Purpose—To evaluate pH-sensitive mixed micelles for multidrug resistant (MDR) ovarian tumor targeting and optical imaging of solid tumors.

Method—Doxorubicin (DOX) encapsulated pH-sensitive mixed micelles composed of poly(L-histidine) (MW 5K)-*b*-PEG(MW 2K) and poly(L-lactic acid)(3K)-*b*-PEG (2K)-folate (PHSM-f) were prepared. Folate receptor-mediated endocytosis, drug uptake, endosomal disruption and cell viability were investigated at the cellular level. For *in vivo* tumor growth inhibition tests, multidrug resistant ovarian A2780/DOX^R xenografted nude mice were used. Optical imaging was performed by using a Cy5.5 fluorescence dye-labeled mixed micelle system. Cy5.5 fluorescence intensity at the tumor site was measured in KB epidermoid xenografted nude mice.

Results—*In vitro* cell viability and drug distribution in the cytoplasm demonstrated the significantly superior efficacy of PHSM-f to free DOX and a control sample of DOX loaded pH-insensitive micelle composed of poly(L-lactic acid)(3K)-*b*-PEG(2K)/poly(L-lactic acid)(3K)-*b*-PEG(2K)-folate (80/20 wt/wt%) (PHIM-f). The mechanisms of these results were proved by folate receptor mediated endocytosis of micelle and endosomal disruption function by it. In addition, the optical imaging demonstrated the future application of the diagnostic area. PHSM-f inhibited the growth of multidrug resistant ovarian tumors efficiently in mice, with minimum weight loss.

Conclusions—The pH-sensitive mixed micelle system demonstrates effective antitumor efficacy against the multidrug resistant ovarian tumor A2780/DOX^R.

Keywords

folic acid; micelle; multidrug resistance; ovarian cancer; poly(L-histidine)

INTRODUCTION

Current tumor chemotherapy faces several challenges that include the lack of tumor selectivity, and intrinsic or acquired drug resistance (1,2). To improve therapeutic efficacy while minimizing side effects, various drug delivery and targeting systems have been investigated

³ To whom correspondence should be addressed. (e-mail: you.bae@utah.edu).

Publisher's Disclaimer: This PDF receipt will only be used as the basis for generating PubMed Central (PMC) documents. PMC documents will be made available for review after conversion (approx. 2–3 weeks time). Any corrections that need to be made will be done at that time. No materials will be released to PMC without the approval of an author. Only the PMC documents will appear on PubMed Central -- this PDF Receipt will not appear on PubMed Central.

such as synthetic polymer-drug conjugates (3), liposomes (4), micelles (5,6), nanogels (7), and micro- or nanosphere (8,9). Nano-sized delivery systems are able to passively accumulate drugs in solid tumors by an enhanced permeation and retention (EPR) effect (10). However, this passive drug delivery system does not guarantee optimal therapeutic efficacy against cancerous tumors when they present multidrug resistance (MDR) (11,12).

Drug release systems triggered in response to local environmental conditions such as temperature (13,14), specific enzymes (15,16), and pH (17–21) seem to be an optional approach to circumvent MDR-associated problems. pH-sensitive drug delivery systems have been used for tumor treatment, utilizing the slightly acidic conditions (pH 6.5–7.2) of the extracellular tumor space (17–21) and the higher acidity in endolysosomal compartments (22). pH-sensitive liposomes (21) are one such delivery system.

Other examples include the polymer-drug conjugate with pH-induced cleavable bonds such as acetal (23,24), hydrozone (25,26), and *N*-ethoxybenzylimidazole bonds (27). These have been used for cytoplasmic drug delivery.

However, the conjugation approach induces a decrease in drug activity because it releases the drug in a harsh lysosomal environment, with high acidity and various enzymes (22). It also often exhibits ill-defined release kinetics and retards the drug release rate, leading to the acquired MDR in a tumor (28).

pH-sensitive polymeric micelles are attractive because of structural destabilization by acidic pH, resulting in rapid drug release (17–21). Specifically, Bae's group has developed pH-sensitive polymeric micelle composed of poly(L-histidine)-*block*-poly(ethylene glycol) (PolyHis(5K)-*b*-PEG(2K)) (17,18). The protonation of polyHis enhances the hydrophilicity below the pK_b of polyHis, while the hydrophobicity is induced by deprotonation above its pK_b. This amphiphilicity enables the formation of polymeric micelles at high pH. PolyHis-*b*-PEG micelles prepared above pH 8.0 by dialysis method are destabilized below pH 7.4.

In addition, a mixed micelle system composed of polyHis-*b*-PEG and poly(L-lactic acid)-*b*-PEG (PLLA-*b*-PEG) increases the stability at pH 7.4 and confers adjustable pH sensitivity through proper composition ratio between polyHis-*b*-PEG and PLLA-*b*-PEG (18). Mixing poly(L-histidine)-*b*-PEG with PLLA-*b*-PEG improved micelle core stability against pH drop due to enhanced hydrophobic interaction in the core. Without PLLA-*b*-PEG mixing the micelle showed instability even at pH 7.4 from previous experience and reports. The drug release profiles affected by the addition of PLLA-PEG were published previously (17). It was proven that PLLA and polyHis in the core are miscible judged by DSC study (29).

Previously, the efficacy of pH-sensitive mixed micelles was proven in *in vitro* and *in vivo* tests using sensitive breast and MDR breast tumor cell lines (17,18).

Figure 1 (a) illustrates the proposed mechanism of pH-sensitive micelles for tumor targeting and Fig. 1 (b) describes the chemical structure of PolyHis-*b*-PEG-folate and PLLA-*b*-PEG-folate. Long-circulating micelles can be extravasated into the tumor area using the EPR effect (10). There are two possible pathways for the micelle after extravasation, depending on the local extracellular tumor pH (~7.0) and the pH range of micelle destabilization (6.8–7.2). One pathway is the micelle destabilization by extracellular tumor acidic pH (~7.0), triggering drug release. The other is folate-receptor mediated endocytosis, which enables micelles internalization into the cell. Both endosomal disruption by polyHis and micelle destabilization due to endosomal acidity can deliver drugs into cytoplasm.

This study provides evidence that folate receptor targeting overcome MDR using resistant A2780/DOX^R xenografts and imaging efficacy using a KB epidermoid xenograft.

MATERIALS AND METHODS

Materials

(3-(4,5-Dimethylthiazol-2-yl)-2,5-diphenyl tetrazolium bromide) (MTT), RPMI 1640, Na₂B₄O₇, triethylamine (TEA), doxorubicin-HCl (DOX·HCl), and dimethylsulfoxide (DMSO) were purchased from Sigma Chemical Co. (St. Louis, USA). Penicillin-streptomycin, fetal bovine serum (FBS), 0.25% (w/v) Trypsin—0.03% (w/v) EDTA solution, and phosphate buffer solution (PBS) were purchased from Gibco Co. (Uxbridge, U.K.). Cy5.5 bis-reactive NHS Ester was purchased from VWR International, Inc. (Aurora, USA). Fluorescein DHPE (*N*-(fluorescein-5-thiocarbonyl)-1,2-dihexadecanoyl-sn-glycero-3-phosphoethanoamine, triethylammonium salt) was purchased from Invitrogen Co. (Eugene, USA). PolyHis(5K)-*b*-PEG(2K) and PLLA(3K)-*b*-PEG(2K)-folate were synthesized as previously described (30, 17).

DOX Loaded Micelle

DOX loaded pH-sensitive mixed micelles (PHSM-f) and pH-insensitive micelles (PHIM-f) were prepared as described before (17,30). Briefly, DOX·HCl was stirred with excess TEA (2× DOX·HCl) in DMSO overnight to obtain a DOX base. The mixed block copolymers (50 mg) were dissolved in 10 ml of DMSO and mixed with a DOX base solution (10 mg DOX base in 10 ml DMSO) and stirred for 3 hr. The solution was transferred to a pre-swollen dialysis membrane (Spectra/Por Molecular weight cut off size 15,000 Da) and dialyzed against NaOH—Na₂B₄O₇ buffer (pH 9.0) for 24 hr at room temperature. The medium was exchanged several times, and the content in the dialysis tube was subsequently lyophilized.

PHSM-f and PHIM-f were composed of polyHis(5K)-*b*-PEG(2K) and PLLA(3K)-*b*-PEG(2K)-folate (80/20 wt/wt%), and PLLA(3K)-*b*-PEG(2K) and PLLA(3K)-*b*-PEG(2K)-folate (80/20 wt/wt%), respectively. The amount of entrapped DOX was determined by HPLC after dissolution in 10% DMSO in methanol. DOX analysis was performed using a Supelco LC-18 column (250×4.6 mm *i.d.*, 5-mm particle size) and an Agilent HPLC instrument. The mobile phase was acetonitrile—0.1% NaH₂PO₄ solution (40:60 v/v%) adjusted to pH 3.0 with H₃PO₄; the flow rate was 1.0 ml/min. DOX was eluted at 6.2 min and detected by fluorescence with excitation wavelength at 480 nm and emission wavelength at 550 nm. The drug loading efficiency of micelles was 75–85 wt %. The DOX loading content was 18 wt%. The average micelle size was 150 nm for PHSM-f and 120 nm for PHIM-f at pH 8.0.

Cell Viability Test

Multidrug resistant ovarian A2780/DOX^R cells (5×10⁴ cells/ml) grown in flasks were harvested with 0.2% (w/v) trypsin—0.1% (w/v) EDTA solution. Two-hundred microliters of cells in RPMI 1640 complete medium was seeded in a 96-well plate and incubated for 1 day. The stock DOX solution (6 mg/ml, pH 7.4) was diluted to prepare the micelle solutions with various DOX concentrations (10–0.0001 mg/ml) for cell cytotoxicity tests. Each solution was diluted with RPMI 1640 cell culture complete medium. The cells were washed three times with PBS (pH 7.4) after 48 hr incubation. Twenty microliters of MTT solution (500 µg/ml) was added to the each well and then incubated for 4 hr. The medium was removed, and DMSO (100 µl) was added to each well for a 10-min incubation. The absorbance of each well was measured with a microplate reader (SpectraMax M2, Molecular Devices, Sunnyvale, CA, USA) at 570 nm.

Hemolysis Test

The hemolytic activity of polyHis-*b*-PEG and PLLA-*b*-PEG was investigated by pH-dependent manners. One SD rat was killed by isoflurane, and blood was obtained by cardiac puncture.

The blood, collected in EDTA-containing tubes, was centrifuged at 1500 *g* for 15 min. The pellet was washed three times with cold PBS (pH 7.4) by centrifugation at 1500 *g* for 15 min at 4°C and was resuspended in the same buffer. Copolymer solutions were added to the erythrocytes solutions (10⁷ cells/mL) at different pHs (pHs 7.4, 7.0, 6.75, and 6.5) and were incubated for 60 min at 37°C in a shaking water bath. The final concentration of the copolymer solution was 1 mg/ml. The release of hemoglobin was determined after centrifugation (1500 *g* for 10 min) by photometric analysis of the supernatant at 541 nm. Complete hemolysis was achieved using 2% Triton X-100, yielding the 100% control value. Zero percent hemolysis was considered as PBS buffer-treated erythrocyte solution (control). Hemolysis (%) of each copolymer was calculated by the following equation.

$$\text{Hemolysis (\%)} = \frac{\text{Abs}_{\text{Sample}} - \text{Abs}_{\text{Control}}}{\text{Abs}_{\text{TritonX-100}} - \text{Abs}_{\text{Control}}} \times 100$$

***In vitro* Confocal Microscopic Study**

To measure the *in vitro* efficacy of mixed micelles, the endosomal disruption by mixed micelles was investigated. The A2780/DOX^R cells grown on Lab-Tek II live cell chamber slides (Nalge Nunc, Naperville, IL, USA) were treated with hydrophobic DHPE fluorescent dye, which encapsulated into the mixed micelle (DHPE/Micelle=1/10 wt/wt% and micelle concentration: 20 µg/ml), and LysoTracker Red DND-99 (80 nM) for 30 min. The encapsulation amount of DHPE inside micelles was measured by using pre-measured DHPE fluorescence calibration curve. The micelle-treated cells were washed three times with PBS (pH 7.4), and the RPMI 1640 medium was replaced with PBS.

Both DHPE fluorescence (green) and lysotracker fluorescence (red) inside live cells were examined by confocal microscopy (Leica TCS NT, Leica, Germany). DHPE dye has a 496 nm excitation and a 519 nm emission wavelength, while lysotracker dye has a 577 nm excitation and a 590 nm emission wavelength.

***In vitro* Flow Cytometry Study**

A2780/DOX^R ovarian cancer cells were cultured in cell culture flasks using RPMI 1640 media supplemented with 10% FBS, 0.4% nistatin, 1.2% insulin, and 1.2% penicillin–streptomycin. Media was changed every other day. The incubator was maintained at 5.0% CO₂ and 36.5°C. The cells (1×10⁶ cells/well) were seeded in a six-well plate, incubated overnight, and harvested with 0.2% (w/v) trypsin—0.1% (w/v) EDTA solution. Two milliliters DOX-loaded micelles with a 20 mg/ml DOX concentration in medium was introduced to each well and incubated for 20 min. The cells were trypsinized, washed three times with PBS solution, and then fixed with 2.5% glutaraldehyde. After filtering through a nylon mesh, cell fluorescence was measured by flow cytometry (FACSCAN, Becton Dickinson) described in details elsewhere (31).

Folate Competition Study

A2780/DOX^R cells were cultured for the cytotoxicity tests, and seeded onto 96-well plates at 5×10⁴ cells/ml, and incubated for 1 day upon seeding. A stock solution containing folate-conjugated micelles loaded with DOX was prepared at a DOX concentration of 1 mg/ml. Another stock solution containing 10 mg/ml of free folic acid was also prepared and filtered through a 0.22-mm pore-size filter. Both solutions were prepared using RPMI growth medium, and a series dilution was then prepared of the stock solution. The previously prepared DOX-loaded micelle solution and free folic acid solutions were subsequently mixed to obtain drug solutions containing 10 µg/ml of DOX and concentrations of free folic acid ranging from 10⁶ µg/ml to 10⁻⁶ µg/ml. The seeded cells were then incubated at 36.5°C with 100 µL of the drug solutions for 2 hr under the presence of 5% CO₂. The cells were then washed once with PBS solution, further incubated with fresh growth medium, and maintained in 5% CO₂, at 37°

C for another 46 hr. The cell viability after incubation with the drug solution was then assessed using the MTT assay as described.

NIR Fluorescence Real-time Tumor Imaging

Cy5.5 (fluorescent dye for *in vivo* imaging) bis-NHS ester (2 mol) was reacted with primary amines of poly(benzyl-His) (MW 5K) (1 mol) in water/DMSO (1 ml/5 ml) mixture solution for 8 hr. After the reaction, unconjugated Cy5.5 bis-NHS ester was removed by dialysis (Molecular cut-off: 8000) for 2 days. Cy5.5 labeled poly(benzyl-His) was lyophilized by freeze-drying. The conjugation of Cy5.5 to the polymer was determined by measuring the extinction coefficient at 675 nm, according to the manufacturer's instructions (Amersham Biosciences co., Piscataway, NJ).

Preparation of Cy5.5 labeled PHSM-f was performed with Cy5.5 labeled poly(benzyl-His), PLLA-*b*-PEG-folate, polyHis-*b*-PEG (10/20/70 wt/wt/wt%) and DOX. 0.9 M NaCl was added to the micelle solution for *in vivo* injection.

For *in vivo* animal experiments, KB tumor cells were inoculated into female nude mice by subcutaneous injection of 1×10^6 cells suspended in cell culture media (RPMI-1640, 10% fetal bovine serum). When the tumor volume in the two injection sites reached 50–70 mm³, 10 mg/kg of equivalent DOX concentration of Cy5.5-labeled micelles was intravenously injected into KB tumor-bearing nude mice through a tail vein.

After *i.v.* administration of Cy5.5 labeled micellar solutions, the time-dependent tissue distribution in tumor-bearing nude mice was imaged by positioning the mice on an animal plate heated to 37°C using the Explore Optix System (ART Advanced Research Technologies Inc., Montreal, Canada). Nude mice were moved to the imaging chamber for scanning. Laser power and count time settings were optimized at 25 mW and 0.3 sec per point. Excitation and emission spots were raster-scanned in 1 mm steps over the selected region of interest to generate emission wavelength scans. A 670 nm pulsed laser diode was used to excite Cy5.5 molecules. Near infrared (NIR) fluorescence emission at 700 nm was detected with a fast photo multiplier tube (Hamamatsu, Japan) and a time-correlated single photon counting system (Becker and Hickl GmbH, Berlin, Germany) (32).

In Vivo Anti-tumor Activity

Five-to 6-week-old female nu/nu nude mice (BALB/c mice) were purchased from Charles River Laboratories (Wilmington, MA, USA). Mice were accommodated in an autoclaved microisolator cage housed in a positive pressure containment rack and maintained under the guidelines of an approved protocol from the University of Utah Institutional Animal Care and Use Committee. They were randomly assigned to experimental and control groups of five or seven animals each. The xenografts of human ovarian A2780/DOX^R MDR carcinoma were developed by subcutaneously implanting 2×10^6 A2780/DOX^R cells in the right flank of the nude mice, as described previously (33). When the tumor volume reached 50–100 mm³, animals were treated three times at 3-day intervals with either DOX-dissolved PBS or DOX encapsulated PHSM-f or PHIM-f micelles. Both formulations were injected intravenously via the mice tail vein at a dose of 10 mg/kg through 25G5/8 needles. The tumor inhibition activity was assessed with the tumor volume size, which was calculated by the following equation: $V = (w)^2 \times (l)/2$, where (*w*) and (*l*) are width and length of the tumor as measured by a caliper. The body weight was measured simultaneously as a side effect of treatment.

RESULTS

In vitro Cell Cytotoxicity and Drug Uptake Test

In vitro results of the cell viability, evaluated by MTT assay, with MDR A2780/DOX^R cells are highlighted in Fig. 2. Free DOX showed almost no toxicity in the tested DOX concentration range (more than 90% viability at 10 µg/mL), suggesting that the cell line has well-developed resistance since DOX resistant A2780 tumor cell line is known to overexpress P-glycoprotein as a major MDR mechanism (34). PHIM-f was slightly more toxic at high concentrations (80% viability at 10 µg/mL) than free DOX.

In contrast, PHSM-f showed clear dose-dependent cytotoxicity, killing approximately 80% of the cell population at 10 µg/ml. Flow cytometry results in Fig. 2(b) show the *in vitro* cellular drug uptake by PHSM-f and PHIM-f with 10-min and 30-min treatments, respectively. There is no significant difference of drug uptake between two micelles at the 10-min time frame. However, significantly higher DOX uptake by PHSM-f than PHIM-f at 30 min was apparent.

This result is consistent with the results of the confocal results in Fig. 2(c). The intracellular drug distribution is illustrated by the measurement of intracellular images. The drug uptake by PHSM-f was initiated at 10 min, while little drug uptake was observed with PHIM-f. At 30 min, confocal microscopy showed a noticeable difference of drug uptake between PHSM-f and PHIM-f. Taken together, the pH-sensitive micelle showed high efficacy of drug delivery inside the cytoplasm of MDR tumor cells.

In vitro Folate Receptor Mediated Endocytosis and Endosomolysis

More than 90% of ovarian carcinomas and most other human tumors have overexpressed folate receptors (35). It is generally accepted that the folate-attached nanoparticles can enter the cells by receptor mediated endocytosis (36). Cellular internalization and tumor specificity through free folate competition test was performed and measured by the MTT assay. Figure 3 (a) shows that the increase in cell viability with an increase of free folic acid concentration was due to the competition between folate ligand conjugate to the micelle and free folic acid toward folate receptors. High free folic acid concentration can prevent the interaction between folate ligand of micelle and folate receptor, leading to low killing efficacy.

In order to elucidate the mechanisms of the *in vitro* results, endosomal disruption by the instinctive fusogenic property of histidine was evaluated using DHPE-encapsulated mixed micelles. Ovarian A2780/DOX^R MDR cell lines were treated with lysotracker fluorescence dye in order to stain the endosome. The tumor cell lines were then treated with micelles. The upper panel in Fig. 3 (b) contains the intracellular confocal images from PHIM-f. Green color represents DHPE fluorescence, and red represents lysotracker labeling.

When cells were treated with DHPE-encapsulated PHIM-f, the green fluorescence DHPE was locally scattered, with limited quantity in the cytoplasm; likewise, lysotracker also was limited in the cytoplasm. However, the confocal image in the lower panel in Fig. 3 (b) illustrates the even distribution of DHPE and lysotracker in the cytoplasm. Although PHIM-f internalized into the tumor cell, the lack of pH-sensitivity and endosomal disruption lead to recycling the endosomes back to the cell surface or degradation in the lysosome (37). In addition, the low fluorescence intensity of Fig. 3 (b) may be due to the DHPE quenching effect by PHIM-f micelle, showing low intracellular PHIM-f. This result indicates that micelles containing His can disrupt the endosomal membrane. Consequently, the encapsulated DHPE was released into the cytoplasm, and the localization of lysotracker and DHPE was prevented. Therefore, histidine containing PHSM-f mediates endosomal membrane disruption and consequent drug delivery in the cytoplasm.

As shown in Fig. 3(c), a hemolysis test evaluated red blood cells (RBC) membrane disruption by polyHis-*b*-PEG and PLLA-*b*-PEG at different pHs. This assay describes the membrane disruption property of polyHis indirectly, using the RBC membrane as an endosomal membrane model (38). The hemolytic activity of polyHis-*b*-PEG was low at pH 7.4, near that of the control sample. Its activity increased as pH decreased but was still low at pH 6.75 (20% lysis). However, at pH 6.5, RBC lysis reached 90%. The hemolytic activity of PLLA-*b*-PEG was lower than 5% at all pHs.

***In Vivo* Biodistribution through Optical Imaging**

The time-dependent excretion of Cy.5.5 and tumor accumulation of pH-sensitive micelle in KB tumor-bearing athymic nude mice were estimated using the eXplore Optix system. The excretion of micelles in live animals was visualized by monitoring real-time near infrared (NIR) fluorescence intensity in the whole body. Figure 4 shows the NIR fluorescence intensities of PHSM-f and PHIM-f. PHSM-f showed significantly higher intensity than PHIM-f up to 24 hr post-injection.

***In vivo* Tumor Growth Inhibition Study and *In Vivo* Body Weight Change**

The growth rates of tumors during the first 9 days were slow and indistinguishable despite various treatments, including control (no treatment). During this time, most animals, with the exception of control animals, lost body weight.

Tumor growth rates deviated from each other after conclusion of the treatments (Days 0, 3 and 6). The volume of tumors treated with PHSM-f was approximately four-fold and five-fold smaller than those treated with PHIM-f and free DOX after 27 days from the first *i.v.* injection (Day 0), respectively. These results show that pH-sensitive mixed micelles inhibit MDR tumors.

The results from the body weight measurement showed that unlike free DOX treatment, there was no serious body weight loss in mice treated with PHSM-f. However, the body weights of mice treated with all formulations recovered after cessation of drug treatment. These results imply that PHSM-f induces less systemic toxicity, probably due to less random drug release in the body, while sustaining micellar integrity.

DISCUSSION

Among gynecological tumors, ovarian cancer is the most fatal in the Western world because most patients (>60%) are diagnosed at an advanced stage of the disease (39,40). Diagnosed patients are typically treated by surgery followed by combination of taxane and platinum-based chemotherapy (41,42). However, most ovarian tumors relapse despite a 65% to 80% initial response rate to first-line chemotherapy. Acquired resistance is responsible for treatment failure, resulting in only 10% to 30% overall 5-year survival rate for late-stage ovarian cancer patients (40).

The mechanistic pH-sensitive dual delivery system is described in Fig. 1(a). Generally, subcutaneous (s.c.) tissue and muscle pHs range from 7.0 to 8.0, with mean values of 7.5 for human s.c. tissue and 7.3 and 7.4 for muscle in dogs and rats, respectively. Malignant tumors show a range of extracellular pH values from 5.8 to 7.6 in human and rodent tumors, respectively. The mean extracellular pH of tumors is 7.0, compared with 7.4 in the blood (43). Due to the variations in extracellular tumor pH, depending on patient, tumor type, and location, the destabilization of pH sensitive mixed micelles is tuned to pH 6.8–7.2 (17,18).

The micelle can release DOX into the extracellular space before being internalized. Interestingly, pretreatment with a drug (paclitaxel or doxorubicin) decreases tumor cell density

and increases interstitial space, consequently promoting the penetration of nanoparticles into three-dimensional tumor histocultures *in vitro* and *in vivo* (44,45). This observation was proposed as a priming effect; if the free drug released into the extracellular space induces the tumor priming effect by killing sensitive cells, this may promote micelle distribution throughout the tumor. However, the lack of free drug (DOX) injection with PHSM-f could be following; 1) free DOX will circulate in the blood stream separated from the micelle and there is low possibility of interactions of the micelles with free DOX, 2) free DOX will cause heart toxicity, and 3) to minimize the number of animals for control experiments.

The folate-attached pH-sensitive micelle system can deliver drugs into the cytoplasm by folate-receptor (FR) mediated endocytosis and endosomolysis, overcoming MDR.

The results in Fig. 2 describe the efficacy of pH-sensitive micelles at the *in vitro* cellular level. The cell viability of free DOX was maintained at 90% to 100%, suggesting that P-glycoprotein (Pgp) in the MDR membrane tumor plays a key role in pumping out drug molecules. PHIM-f showed 80% of cell viability even at the highest DOX concentration (10 $\mu\text{g/ml}$), indicating that the endosomal escape of PHIM-f is the principal deficiency of drug delivery into the cytoplasm, despite cellular internalization by active endocytosis.

In contrast, FR-mediated endocytosis and drug release into the cytoplasm by endosomal escape enables PHSM-f to have the highest tumor cell killing efficiency. The cell viability results were confirmed by drug uptake, as seen in Fig. 2(b) and (c).

To further support the function of micelles, three tests were conducted: free folate competition, intracellular localization, and hemolysis. In Fig. 3(a), the viability of the cells treated with PHSM-f was proportional to the free folic acid concentration in the cell culture medium up to 10^{-2} $\mu\text{g/ml}$, suggesting that active uptake is required for MDR treatment. However, viability is almost 100% at more than 10^{-1} $\mu\text{g/ml}$ of free folic acid. Clinically, the plasma folate concentration in humans is lower than 0.003 $\mu\text{g/ml}$ (46), suggesting that PHSM-f interacts with the folate receptor of tumor cells when systemically administrated.

The confocal image in Fig. 3(b) supports that the dye carried by the PHSM-f micelle exits out of the endolysosomal compartment. In addition, the hemolysis results also confirm endosomal disruption property by polyHis. In Fig. 3(c), the hemolysis study demonstrates endosomal membrane disruption by polyHis at low pH (6.5). Because anionic lipids are known to be located on the cytoplasmic side of the plasma and endosomal membrane, positively charged polyHis at pH 6.5 could fuse and destabilize the RBC membrane. Due to the fusogenic property of polyHis, the pH-sensitive micelle composed of histidine could escape endosome.

Figure 4 illustrates the utilization of *in vivo* optical tumor imaging using pH-sensitive micelles. NIR fluorescence described the tumor targeting and tumor accumulation efficacy; NIR fluorescence intensity of PHSM-f was 1.5-fold higher than PHIM-f, which is consistent with the results from Figs. 2 and 3. From this result, the pH-sensitive micelle is likely to be useful for diagnostic imaging application. Finally, *in vivo* tumor growth inhibition tests (Fig. 5) confirmed the efficacy of pH-sensitive micelles for tumor targeting.

CONCLUSION

These promising results from our study prove the antitumor efficacy of pH-sensitive micelles using polyHis at the *in vitro* cellular level and *in vivo*. Cellular internalization through ligand receptor mediated endocytosis, endosomolysis through endosomal membrane disruption, and pH sensitive drug release enable micelles to inhibit tumors effectively and to be useful for non-invasive diagnostic imaging. Taken together, pH-sensitive micelles composed of His have a promising future in clinical applications.

ACKNOWLEDGMENT

This work was partially supported by NIH CA 101850. Drs. Zhonggao Gao, Kyung Taek Oh, and Han Chang Kang are acknowledged for their help with various experiments.

REFERENCE

1. Brannon-Peppas L, Blanchette JO. Nanoparticle and targeted systems for cancer therapy. *Adv. Drug Deliv. Rev* 2004;56:1649–1659. [PubMed: 15350294]
2. Szakacs G, Paterson JK, Ludwig JA, Booth-Genthe C, Gottesman MM. Targeting multidrug resistance in cancer. *Nat. Rev. Drug Discov* 2006;5:219–234. [PubMed: 16518375]
3. Duncan R. Drug-polymer conjugates: potential for improved chemotherapy. *Anticancer Drugs* 1992;3:175–210. [PubMed: 1525399]
4. Torchilin VP. Liposomes as targetable drug carriers. *Crit. Rev. Ther. Drug Carr. Syst* 1985;1:65–115.
5. Jones M, Leroux J. Polymeric micelles—a new generation of colloidal drug carriers. *Eur. J. Pharm. Biopharm* 1999;48:101–111. [PubMed: 10469928]
6. Kwon GS, Kataoka K. Block copolymer micelles as long circulating drug vehicles. *Adv. Drug Deliv. Rev* 1995;16:295–309.
7. Vinogradov SV, Bronich TK, Kabanov AV. Nanosized cationic hydrogels for drug delivery: preparation, properties and interactions with cells. *Adv. Drug Deliv. Rev* 2002;54:135–147. [PubMed: 11755709]
8. Okada H, Toguchi H. Biodegradable microspheres in drug delivery. *Crit. Rev. Ther. Drug Carr. Syst* 1995;12:1–99.
9. Carino GP, Jacob JS, Mathiowitz E. Nanosphere based oral insulin delivery. *J. Control. Release* 2000;65:261–269. [PubMed: 10699286]
10. Maeda H. The enhanced permeability and retention (EPR) effect in tumor vasculature: the key role of tumor-selective macromolecular drug targeting. *Adv. Enzyme Regul* 2001;41:189–207. [PubMed: 11384745]
11. Larsen AK, Escargueil AE, Skladanowski A. Resistance mechanisms associated with altered intracellular distribution of anticancer agents. *Pharmacol. Ther* 2000;88:217–229. [PubMed: 10739876]
12. Bennis S, Chapey C, Couvreur P, Robert J. Enhanced cytotoxicity of doxorubicin encapsulated in polyhexylcyanoacrylate nanospheres against multi-drug-resistant tumor cells in culture. *Eur. J. Cancer A* 1994;30:89–93. [PubMed: 8142172]
13. Cammas S, Suzuki K, Sone C, Sakurai Y, Kataoka K, Okano T. Thermo-responsive polymer nanoparticles with a core-shell micelle structure as site-specific drug carriers. *J. Control. Release* 1997;48:157–164.
14. Chung JE, Yokoyama M, Okano T. Inner core segment design for drug delivery control of thermo-responsive polymeric micelles. *J. Control. Release* 2000;65:93–103. [PubMed: 10699274]
15. Kopecek J, Kopeckova P, Minko T, Lu Z. HEMA copolymer—anticancer drug conjugates: design, activity, and mechanism of action. *Eur. J. Pharm. Biopharm* 2000;50:61–81. [PubMed: 10840193]
16. Putnam D, Kopecek J. Enantioselective Release of 5-Fluorouracil from N-(2-Hydroxypropyl) methacrylamide-Based Copolymers via Lysosomal Enzymes. *Bioconjug. Chem* 1995;6:483–492. [PubMed: 7578369]
17. Lee ES, Na K, Bae YH. Polymeric micelle for tumor pH and folate-mediated targeting. *J. Control. Release* 2003;91:103–113. [PubMed: 12932642]
18. Lee ES, Na K, Bae YH. Doxorubicin loaded pH-sensitive polymeric micelles for reversal of resistant MCF-7 tumor. *J. Control. Release* 2005;103:405–418. [PubMed: 15763623]
19. Lee ES, Na K, Bae YH. Super pH-sensitive multifunctional polymeric micelle. *Nano Lett* 2005;5:325–329. [PubMed: 15794620]
20. Gillies ER, Frechet JM. pH-responsive copolymer assemblies for controlled release of doxorubicin. *Bioconjug. Chem* 2005;16:361–368. [PubMed: 15769090]
21. Drummond DC, Zignani M, Leroux JC. Current status of pH-sensitive liposomes in drug delivery. *Prog. Lipid Res* 2000;39:409–460. [PubMed: 11082506]

22. Duncan R. Polymer conjugates for tumour targeting and intracytoplasmic delivery. The EPR effect as a common gateway? *Pharm. Sci. Technol. Today* 1999;2:441–449. [PubMed: 10542390]
23. Gillies ER, Jonsson TB, Frechet JM. Stimuli-responsive supramolecular assemblies of linear-dendritic copolymers. *J. Am. Chem. Soc* 2004;126:11936–11943. [PubMed: 15382929]
24. Tomlinson R, Heller J, Brocchini S, Duncan R. Polyacetal-doxorubicin conjugates designed for pH-dependent degradation. *Bioconjug. Chem* 2003;14:1096–1106. [PubMed: 14624622]
25. Hruby M, Konak C, Ulbrich K. Polymeric micellar pH-sensitive drug delivery system for doxorubicin. *J. Control. Release* 2005;103:137–148. [PubMed: 15710507]
26. Bae Y, Fukushima S, Harada A, Kataoka K. Design of environment-sensitive supramolecular assemblies for intracellular drug delivery: polymeric micelles that are responsive to intracellular pH change. *Angew. Chem. Int. Ed. Eng* 2003;42:4640–4643.
27. Kong SD, Luong A, Manorek G, Howell SB, Yang J. Acidic hydrolysis of *N*-ethoxybenzylimidazoles (NEBIs): potential applications as pH-sensitive linkers for drug delivery. *Bioconjug. Chem* 2007;18:293–296. [PubMed: 17261055]
28. Hahn SM, Russo A, Cook JA, Mitchell JB. A multidrug-resistant breast cancer line induced by weekly exposure to doxorubicin. *Int. J. Oncol* 1999;14:273–279. [PubMed: 9917502]
29. Yin H, Lee ES, Kim D, Lee KH, Oh KT, Bae YH. Physicochemical characteristics of pH-sensitive poly(L-Histidine)-*b*-poly(ethylene glycol)/poly(L-Lactide)-*b*-poly(ethylene glycol) mixed micelles. *J. Control. Release* 2008;126:130–138. [PubMed: 18187224]
30. Lee ES, Shin HJ, Na K, Bae YH. Poly(L-histidine)-PEG block copolymer micelles and pH-induced destabilization. *J. Control. Release* 2003;90:363–374. [PubMed: 12880703]
31. Gao ZG, Fain HD, Rapport N. Ultrasound-enhanced tumor targeting of polymeric micellar drug carriers. *Mol. Pharmacol* 2004;1:317–330.
32. Park K, Kim JH, Nam YS, Lee S, Nam HY, Kim K, Park JH, Kim IS, Choi K, Kim SY, Kwon IC. Effect of polymer molecular weight on the tumor targeting characteristics of self-assembled glycol chitosan nanoparticles. *J. Control. Release* 2007;122:305–314. [PubMed: 17643545]
33. Gao ZG, Fain HD, Rapport N. Controlled and targeted tumor chemotherapy by micellar-encapsulated drug and ultrasound. *J. Control. Release* 2005;102:203–222. [PubMed: 15653146]
34. Spoelstra EC, Dekker H, Schuurhuis GJ, Broxterman HJ, Lankelma J. P-glycoprotein drug efflux pump involved in the mechanisms of intrinsic drug resistance in various colon cancer cell lines: evidence for a saturation of active daunorubicin transport. *Biochem. Pharmacol* 1991;41:349–359. [PubMed: 1671638]
35. Lu Y, Low PS. Immunotherapy of folate receptor-expressing tumors: review of recent advances and future prospects. *J. Control. Release* 2003;91:17–29. [PubMed: 12932634]
36. Lu Y, Low PS. Folate-mediated delivery of macromolecular anticancer therapeutic agents. *Adv. Drug Deliv. Rev* 2002;54:675–693. [PubMed: 12204598]
37. Mohajer G, Lee ES, Bae YH. Enhanced intracellular retention activity of novel pH-sensitive polymeric micelles in wild and multidrug resistant MCF-7 cells. *Pharm. Res* 2007;24:1618–1627. [PubMed: 17385015]
38. Jones RA, Cheung CY, Black FE, Zia JK, Stayton PS, Hoffman AS, Wilson MR. Poly(2-alkylacrylic acid) polymers deliver molecules to the cytosol by pH-sensitive disruption of endosomal vesicles. *Biochem. J* 2003;372:65–75. [PubMed: 12583812]
39. Jemal A, Siegel R, Ward E, Murray T, Xu J, Smigal C, Thun MJ. Cancer statistics. *CA Cancer J. Clin* 2006;56:106–130. [PubMed: 16514137]
40. Cannistra SA. Cancer of the ovary. *N. Engl. J. Med* 2004;351:2519–2529. [PubMed: 15590954]
41. du Bois A, Quinn M, Thigpen T, Vermorken J, Avall-Lundqvist E, Bookman M, Bowtell D, Brady M, Casado A, Cervantes A, Eisenhauer E, Friedlaender M, Fujiwara K, Grenman S, Guastalla JP, Harper P, Hogberg T, Kaye S, Kitchener H, Kristensen G, Mannel R, Meier W, Miller B, Neijt JP, Oza A, Ozols R, Parmar M, Pecorelli S, Pfisterer J, Poveda A, Provencher D, Pujade-Lauraine E, Randall M, Rochon J, Rustin G, Sagae S, Stehman F, Stuart G, Trimble E, Vasey P, Vergote I, Verheijen R, Wagner U. consensus statements on the management of ovarian cancer: final document of the 3rd International Gynecologic Cancer Intergroup Ovarian Cancer Consensus Conference (GCIG OCCC 2004). *Ann. of Oncol* 2004;2005;16(Suppl 8):viii7–viii12. [PubMed: 16239238]

42. McGuire WP III. Current status of taxane and platinum-based chemotherapy in ovarian cancer. *J. Clin. Oncol* May 15;2003 21(Suppl):133s–135s. [PubMed: 12743128]
43. Wike-Hooley JL, Haveman J, Reinhold JS. The relevance of tumor pH to the treatment of malignant disease. *Radiother. Oncol* 1984;2:343–366. [PubMed: 6097949]
44. Jang SH, Wientjes MG, Au JL. Enhancement of paclitaxel delivery to solid tumors by apoptosis-inducing pretreatment: effect of treatment schedule. *J. Pharmacol. Exp. Ther* 2001;296:1035–1042. [PubMed: 11181938]
45. Jang SH, Wientjes MG, Lu D, Au JL. Drug delivery and transport to solid tumors. *Pharm. Res* 2003;20:1337–1350. [PubMed: 14567626]
46. Haidemenos A, Kontis D, Gazi A, Kallai E, Allin M, Lucia B. Plasma homocysteine, folate and B12 in chronic schizophrenia. *Prog. Neuro-psychopharmacol. Biol. Psychiatry* 2007;31:1289–1296.

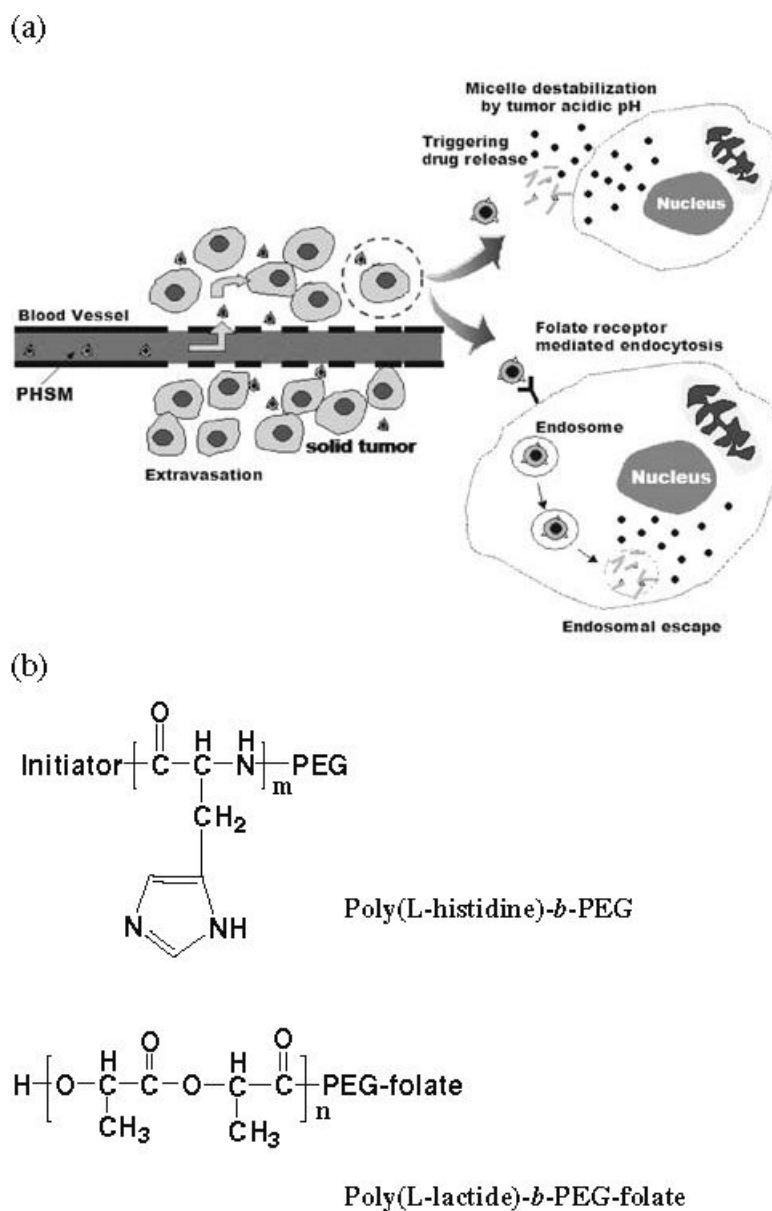


Fig. 1. (a) Schematic picture describing the mechanism of pH sensitive micelles (PHSM-f) for tumor targeting and (b) chemical structures of poly(L-histidine)-*b*-PEG and PLLA-*b*-PEG-folate.

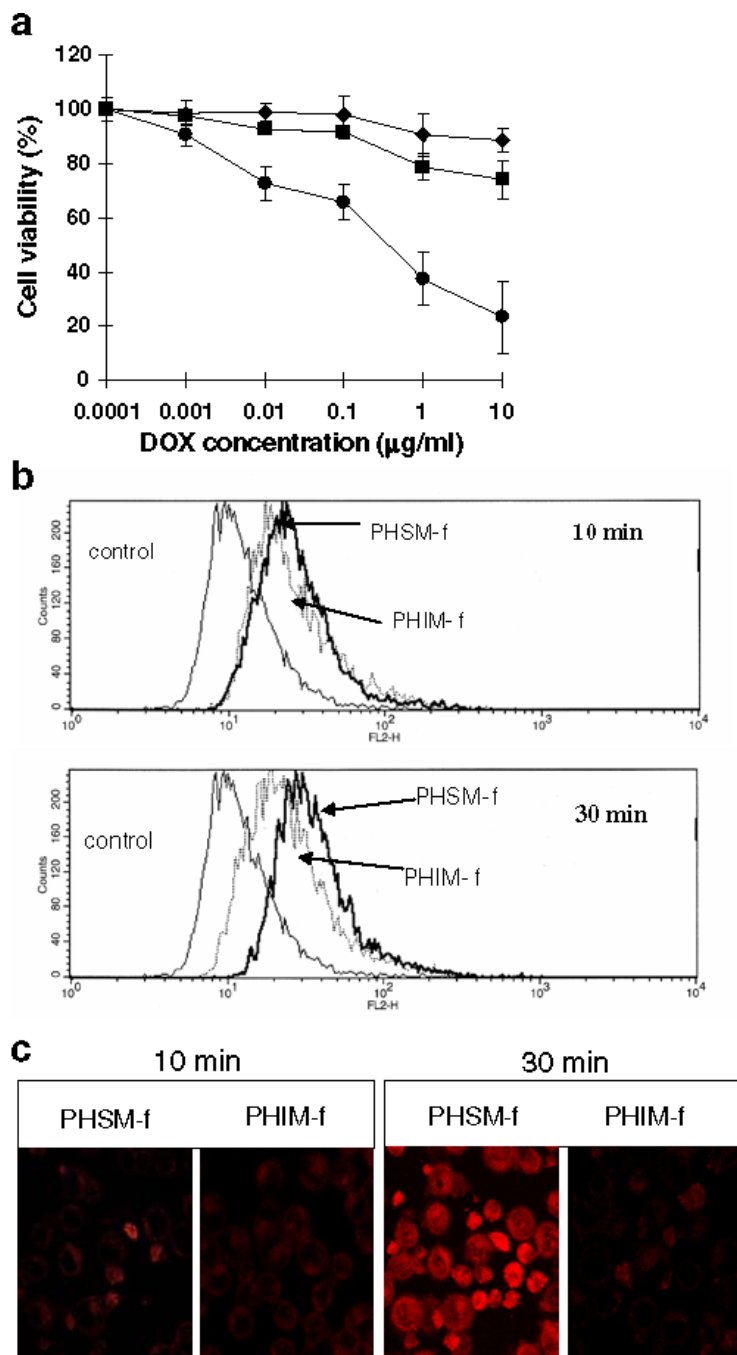


Fig. 2. (a) The cytotoxicity of free DOX (◆), DOX loaded pH-sensitive mixed micelle with folate (PHSM-f) (●), and pH-insensitive micelle with folate (PHIM-f) (■), against ovarian A2780/DOX^R tumor cells after 48 hr incubation ($n=9$). (b) Flow cytometry analysis of drug uptake by PHSM-f and PHIM-f for 10 min or 30 min followed by incubation in fresh medium for 2 hr. (c) Confocal images of ovarian A2780/DOX^R tumor cells treated with PHSM-f and PHIM-f for 10 min and 30 min treatment followed by 4 hr incubation with RPMI 1640 media after micelle removal.

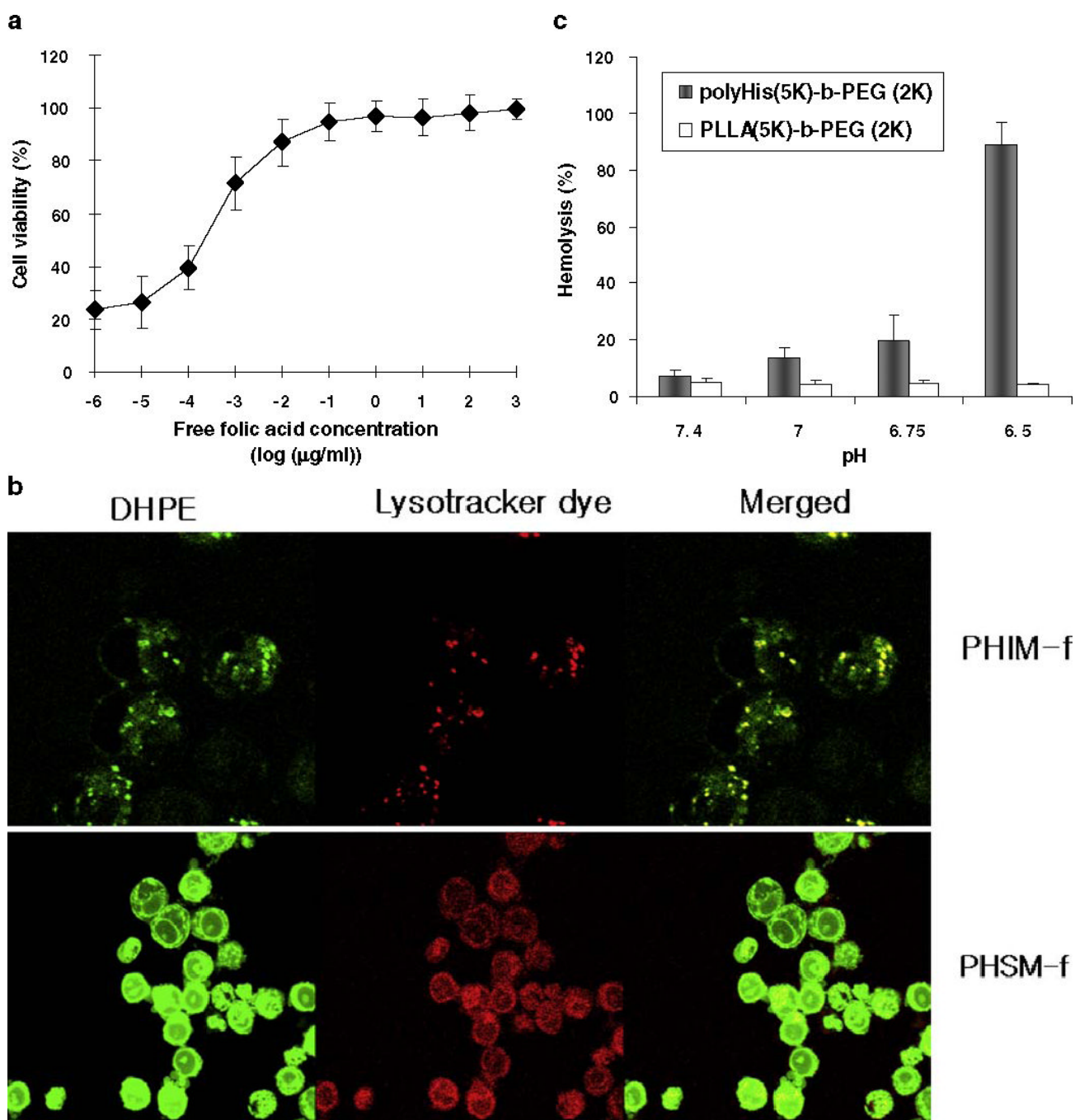


Fig. 3. Mechanistic *in vitro* cellular tests: **(a)** Cell viability after incubation of A2780/DOX^R MDR tumor cell lines with DOX encapsulated PHSM-f and free folic acid (10^6 μg/ml to 10^{-6} μg/ml of free folic acid concentration) at 10 μg/ml of DOX; **(b)** *In vitro* endosomal disruption using lysotracker dye and fluorescein DHPE encapsulated PHSM-f and PHIM-f; **(c)** Hemolytic effects of polyHis-b-PEG and PLLA-b-PEG with different pHs at a copolymer concentration of 1 mg/ml. (mean ± SD, $n=7$).

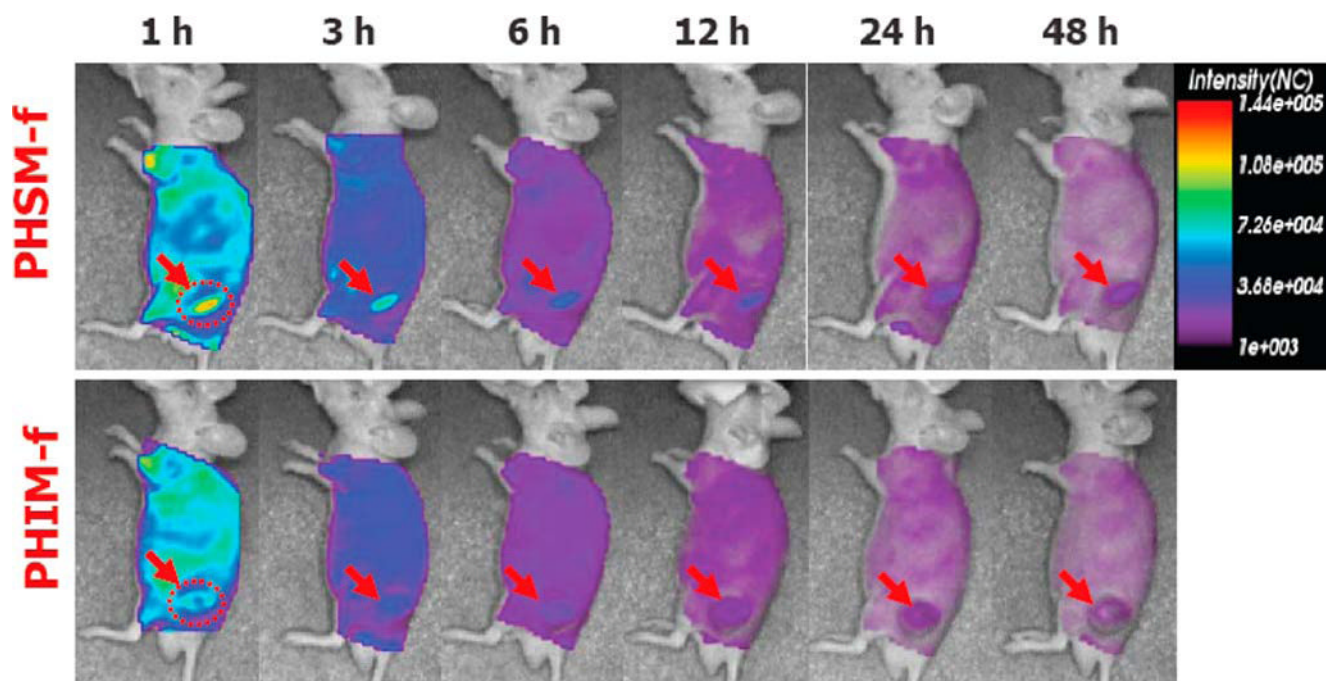


Fig. 4.
In vivo optical fluorescence imaging of KB tumor xenografted athymic nude mice post DOX encapsulated and Cy5.5 fluorescent dye labeled PHSM-f and PHIM-f. Arrows specifies the location of tumor.

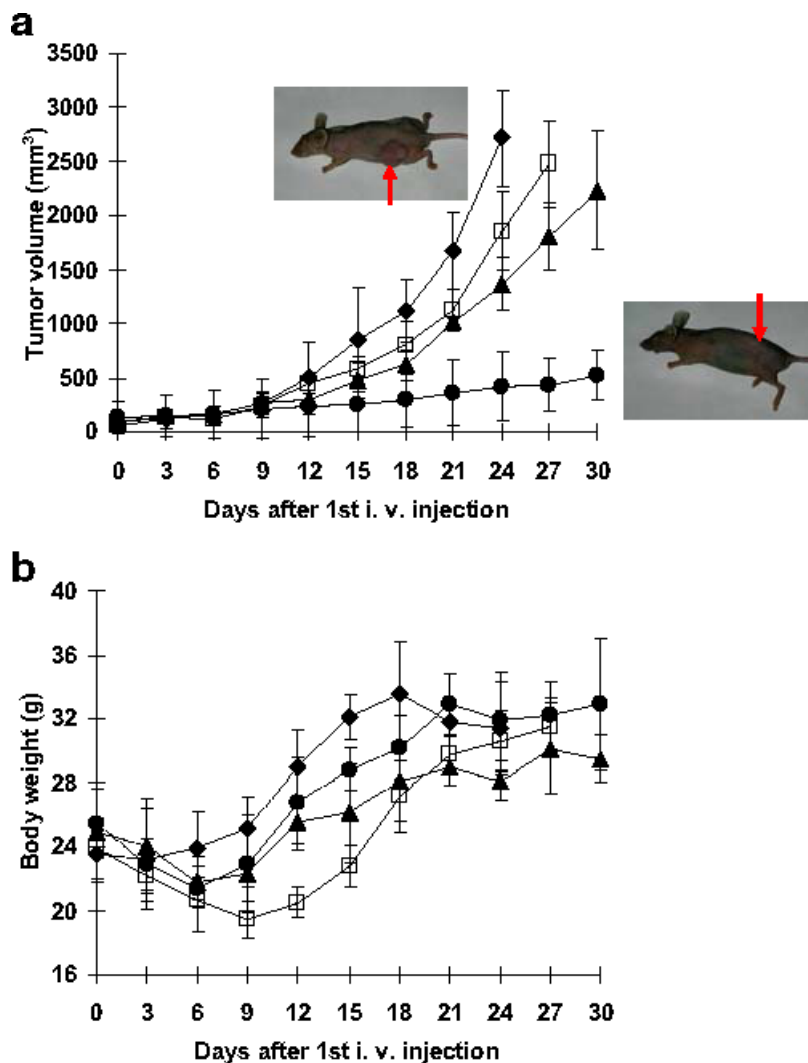


Fig. 5. Tumor growth inhibition test and body weight change of *s.c.* ovarian A2780/DOX^R xenografts in BALB/c nude mice ($n=7$). Mice were injected *i.v.* with 10 mg/kg DOX equivalent dose: DOX loaded PHSM-f (●), PHIM-f (▲), free DOX (□), and control (◆). Three *i.v.* injections on days 0, 3, and 6 were made. Values are the mean \pm standard deviation (S.D.). (a) Tumor volume change (b) body weight changes. The animal pictures were taken after 30 days and an arrow indicates the tumor.